Journal of Geography, Environment and Earth Science International

Volume 27, Issue 9, Page 1-18, 2023; Article no.JGEESI.102580
ISSN: 2454-7352

Dust Outbreaks across East Iran: Application of Multi-Source Remote Sensing Data (AMSR-E and FengYun3-MWRI) on the Effects of Soil Moisture

Abouzar Mehraban [a], Yansong Bao [b], Emmanuel Yeboah [c*], Benedicta Akua Sarfo [d], Michael Kpakpo Allotey [e], Charafa El Rhadiouini [c], Ben Emunah Aikins [f], Desmond Nii Ayitey Mettle-Nunoo [g], Michael Atuahene Djan [h], Abraham Okrah [i] and Isaac Sarfo [j,k]

[a] Institute of Remote Sensing, Nanjing University of Information Science and Technology, 210044 Nanjing, Jiangsu, China.
[b] Key Laboratory for Aerosol Cloud Precipitation, College of Atmospheric Physics, Nanjing University of Information Science and Technology, 210044 Nanjing, Jiangsu, China.
[c] School of Remote Sensing and Geomatics Engineering, Nanjing University of Information Science and Technology, 210044 Nanjing, Jiangsu, China.
[d] University of Ghana Business School (UGBS), University of Ghana, Legon, Ghana.
[e] Department of Geography and Resource Development, University of Ghana, Legon, Ghana.
[f] Bedeston Technologies and Consultancy Services Limited, Accra, Ghana.
[g] Department of Information Studies, University of Ghana, Legon, Ghana.
[h] Department of Geography and Environmental Studies, New Mexico State University, United States of America.
[i] Collaborative Innovation Center on Forecast and Evaluation of Meteorological Disaster, Nanjing University of Information Science and Technology, 210044 Nanjing, Jiangsu, China.
[j] College of Geography and Environmental Science, Henan University, 475000 Kaifeng, Henan Province, China.
[k] Organization of African Academic Doctors (OAAD), Off Kamiti Road, P.O. Box 25305000100, Nairobi, Kenya.

Authors' contributions

This work was carried out in collaboration among all authors. All authors read and approved the final manuscript.

Article Information

DOI: 10.9734/JGEESI/2023/v27i9702

Open Peer Review History:
This journal follows the Advanced Open Peer Review policy. Identity of the Reviewers, Editor(s) and additional Reviewers, peer review comments, different versions of the manuscript, comments of the editors, etc are available here: https://www.sdiarticle5.com/review-history/102580

**Corresponding author: E-mail: 202251110001@nuist.edu.cn;*

Original Research Article

Received: 11/05/2023
Accepted: 13/07/2023
Published: 25/07/2023

ABSTRACT

One of the most significant hydro-meteorological and agricultural variables is soil moisture, yet measuring it remains a difficult task. Due to the significant spatial fluctuation of soil moisture, it is difficult to quantify it in a particular spot or field across a sizable region. Despite the thermal band's limitations in assessing soil moisture, MODIS and AVHRR, which are inappropriate were utilized in this investigation. The study examined the impact of soil moisture on dust outbreak. Soil moisture in the study domain was monitored using field techniques and the hybrid model. It combined multi-sourced remote sensing data, obtained from AMSER-E and FY-3 satellites. AMSER-E satellite measures the light temperature in five frequencies ranging from 6. 9 to 89 GHz based on data obtained from AMSER-E. Findings revealed areas with a spatial scale of 25 km^2 has a 12-hour time step or variability in dust storm, thereby influencing soil moisture content within the zone of study. In addition to introducing acceptable potentials of the passive microwave band for accurate and applied monitoring of the soil moisture, the present results are viewed as a reliable source for studies on drought in time scale. The study shows that Zabol in Sistan has the highest annual average of 80.7 dust storm days. Soil moisture estimates serve a great deal for preparing soil moisture maps and the evaluation of temporal and spatial variations of soil moisture in study region to address issues related to dust storms.

In order to identify the areas affected by dust storms and understand how dust particles are dispersed in the Sistan region, satellite image processing was employed using MODIS 1 sensor images obtained from the TERRA satellite.

Keywords: AMSER-E; FY-3; soil moisture; dust; Zabol; Iran; Khorasan Razavi.

1. INTRODUCTION

Dust storms are one category of major environmental issue. Dust storms are a severe meteorological phenomenon that lowers the air, reduces horizontal sight to less than 1 km, and creates a powerful, violent wind that propels small dust particles and winds from the ground. Most dust storms develop close to desert terrain. Eastern Iran's dust was flung southward, passing through several regions of the Lut plain. Sand and dust mobilization in dust-source locations has been ascribed mostly to humidity and wind speed. However, in addition to wind speed, surface characteristics also have a bearing on dust occurrences [1-5]. Except in freezing temperatures or when there are coarse grey soils present, surface elements such as soil moisture dictate the friction threshold velocity for the release of dust in bare soil. This is due to soil moisture's amplification of the fusion forces between soil particles [6-9]. Consequently, under very wet conditions, wet sand needs significant wind speed to generate a dust event. Many efforts have been made in laboratories and through observations to elucidate the mechanisms of dust emissions from moistened sand [10-14]. Nevertheless, the estimation of the association between soil moisture and dust storms is only partially supported by this research. Employing satellite-based and global assimilation data would be necessary to understand the mechanisms relating dust events and soil moisture trends on a global scale and for natural dust occurrences [15-19].

One of the most significant hydro-meteorological and agricultural variables is soil moisture, yet measuring it remains a difficult task. Due to the significant spatial fluctuation of soil moisture, it is difficult to quantify it in a spot or field across a sizable region [20-24]. To accurately forecast changes in the local water balance, it is crucial to assess the soil moisture, which is a crucial step in the water cycle [25-29]. Due to the necessity for soil moisture to make nutrients soluble for plant absorption, spatial variations in soil moisture might vary in terms of low or varied locations in agricultural production. Due to various site-specific geology and climatic

circumstances, including soil type, soil horizon, and other factors, soil moisture varies both geographically and temporally. Traditional efforts to measure soil moisture have been principally restricted to in situ measurements. High wind speeds on the ground surface promote this because soil moisture levels are directly linked to precipitation, which decreases the soil's permeability and diminishes vegetative cover [30-33]. In recent years, soil moisture has been extensively monitored using microwave sensors. The accuracy of the findings received from the data is significantly influenced by the choice of the best measuring method and the most suitable band. Despite the thermal band's limitations in assessing soil moisture, MODIS and AVHRR—which are inappropriate—are used most frequently in this area of research. In view of this study which examined the impact of soil moisture on dust outbreak. Soil moisture in this study domain was monitored using field techniques and the hybrid model. It combined multi-sourced remote sensing data, obtained from AMSER-E and FY-3 satellites. This study draws attention on the usefulness of soil moisture in regulating dust storms, hence, measurement of the said component or variable either from a specific spot or across large areas remain a daunting task which calls for in-depth analyses in this regard [34-38].

While satellite remote sensing of dust has become more accessible and has shown promising and reliable results in recent years, in situ measurements of dust aerosol characteristics and dust loading are still deemed essential. Therefore, several campaigns have been carried out in arid regions worldwide, with a primary focus on the Sahara, which is the largest and most active dust source region [39-41]. Despite the significant dust activity and plume exposures extending from the Sahara to the Atlantic and Mediterranean regions, fewer studies have been conducted in the Middle East and southwest Asia.

Sistan stands out as one of the highly active dust source regions in southwest Asia. Following a period of drought in the 1990s, there has been an observed increase in the occurrence of dust storms. Additionally, the Hamoun region contributes significantly to dust emissions, leading to the deterioration of air quality in the area. The amount of dust is influenced by factors such as the intensity and duration of the storms, their altitude, and the distance from the source. However, a crucial factor in dust generation is the soil surface moisture, which plays a vital role in determining the extent of dust emissions [42-44].

The Sistan region, situated between 30°5′ N–31°28′ N and 61°15′ E–61°50′ E, is located in the southeastern part of Iran, near the Iranian borders with Pakistan and Afghanistan. The region comprises four cities and 980 villages, with a population exceeding 400,000. Its climate is characterized as arid, with an average annual precipitation of 55 mm, primarily occurring during the winter months (December to February). Due to high temperatures, the evaporation rate surpasses approximately 4000 mm per year (Moghaddamnia et al., 2009).

2. MATERIALS AND METHODS

2.1 Description of Conditions in the Study Region

Sistan is located in the eastern part of Iran, specifically in the northern region of the Sistan and Baluchestan province (Fig. 1). The city of Zabol, with a population of over 300,000, is situated approximately 215 km away from Zahedan City, which serves as the provincial capital. In recent times, Zabol City has been identified as one of the areas affected by windborne dust deposition during periods of drought. The Sistan region, due to its geographical location, experiences various monsoon winds, with the most notable being the 120-day winds. These winds typically begin in late May and persist until mid-September, significantly influencing temperature moderation in the region. The Sistan plain is covered by quaternary sediments primarily composed of clay and sand, which are highly susceptible to wind erosion.

The sole naturally occurring feature in the Khajeh Mountain region of Kost Rostam is the Sistan altitudes with the north-south axis, which includes compressive folds that extend from the west to the Lut desert and from the east to the Sistan plain. The region's primary economic mainstays, agriculture and livestock, are complemented by a few rural enterprises including carpet weaving, tie and dye, petty trading and so on. Wheat, barley, cereals, as well as some fruits and vegetables, are among the crop items grown in the surrounding areas. The importance of agriculture in the area and other outlying towns is matched by the relevance of livestock breeding and animal husbandry, which are the primary activities around the Hamoon Lake.

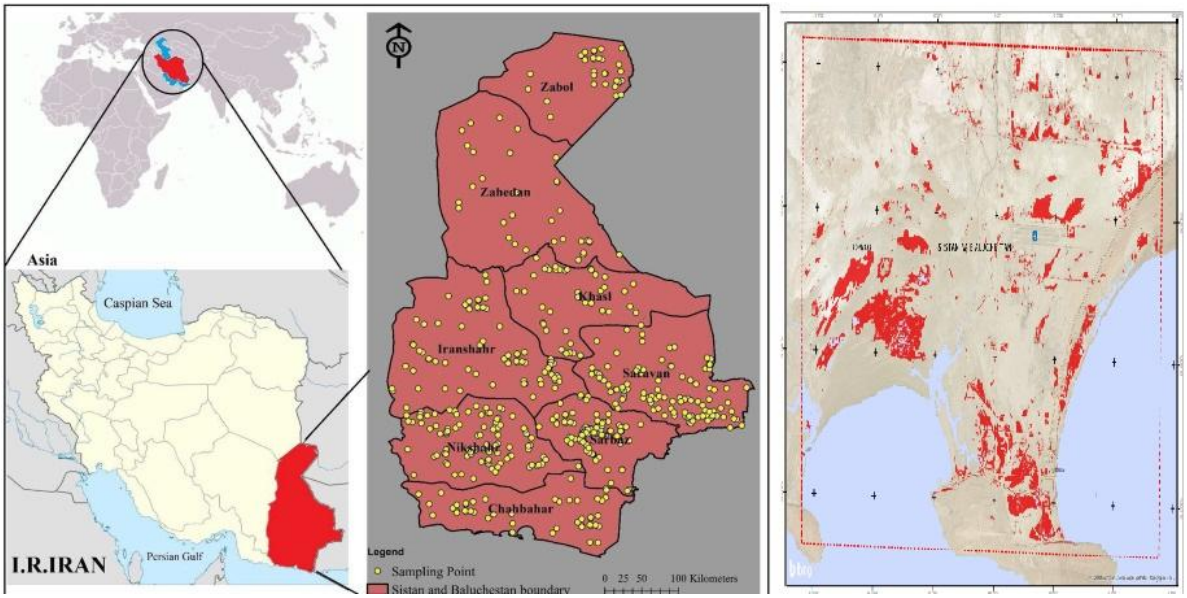

Fig. 1. The location of the study area for dust on a 3D satellite image

2.2 Datasets

The data and information utilized in this research can be categorized into two main groups. The first group comprises spatial information, which includes satellite images and topographical maps. The satellite images are in digital format and encompass data from AMSR-E and FengYun3-MWRI images spanning the years 2013 to 2017, corresponding to the period when the storms occurred. The second group consists of descriptive information, which incorporates ground data obtained from weather stations located in the region.

In order to identify the areas affected by dust storms and understand the dispersion of dust particles, satellite image processing has been employed in the Sistan region. Dust storms in this region cover a wide area and can transport dust particles to distant locations. Therefore, the identification of these storms requires the use of images with high coverage and reproducibility. The MODIS 1 sensor from the TERRA satellite possesses these desired characteristics. Furthermore, the sensor is capable of capturing a broad range of radiant energy in both visible and invisible spectral ranges, making it well-suited for the intended purposes.

In most cases, soil moisture retrieval is performed at three different earth depth levels. Using satellite passive microwave such as AMSER-E and FY3B-MWRI satellites and ground-based observational data. Satellite data should be calibrated using field observational data. It should be considered to eliminate rainy days' data or corrupted data. That includes the following steps:

2.3 Meteorology Data

Products such as wind speed (WS) at 10.0 m height, volumetric soil moisture (VSM), and soil temperature at a depth of 0–10.0 cm, and rainfall rate will be used from meteorology stations. There are more than 100 meteorological stations which are primarily automatic and synoptic in the study area.

2.3.1 Soil moisture data preprocessing

Significant differences were observed in the data collected for the soil moisture content from different units. P-value (0.769) was found using the Dixon's test and was more than the significance level of 0.05 alpha, allowing soil moisture data to be taken into account without flood data. Atmospheric and geometric corrections for FY-3 images were performed. Regarding the smoothness (at least 1214 and maximum 1500 meters above sea level) and the lack of high topographic conditions in the study area, the ATCOR2 model was used as the absolute atmospheric correction (for geometric corrections of ground-corrected reflecting data from Google data). In this investigation, the inheritance was employed, and the desired root means square error was 0.622 pixels. By comparing it to GPS data and doing geometric

adjustments on mid-scale imagery like Thematic Mapper, Google Earth data shows that the square root mean square deviation of 0.00014 is accurate.

2.3.2 AMSER-E satellite imagery

In this study, the data obtained from AMSR-E-EOS of NASA were utilized. Products of the soil moisture have been elicited from AMSR-E/Aqua Daily L3 Surface Soil Moisture, Interpretive Parameters, & QC EASE-Grids ascending and describing data. This series of images has been prepared for a 1-year statistical period (Since the beginning of January 2009 until the beginning of January 2010) at a spatial resolution of 25 Km^2 and a 12-hour time step. AMSR-E on NASA's EOS Aqua satellite was launched on May 4 2002, and had operated until October 4 2011.

As the successor to AMSR-E, AMSR2 on-board the sun-synchronous satellite GCOM-W1 was launched on 18 May 2012 by JAXA. GCOM-W1 is the first of three planned satellites of the GCOM-W project, which is a 13-year mission designed for global and continuous observation of Earth's water and energy cycles. AMSR2 has most of the characteristics of AMSR-E. Both sensors are conical scanning passive microwave radiometers with similar instrument configurations. The AMSR instruments measure microwave emissions from the earth surface twice daily for descending/ascending orbital equatorial crossings at 1:30 AM/PM local time, with vertically (V) and horizontally (H) polarized Tb retrievals at six frequencies (6.9, 10.7, 18.7, 23.8, 36.5, 89.0 GHz). Major changes in AMSR2, distinctive from AMSR-E, include an additional frequency at 7.3 GHz designed for mitigating Radio Frequency Interference (RFI), and a larger (2.0 m diameter) main reflector for enhanced spatial resolution. The MWRI onboard the FY-3B satellite was launched 5 November 2010. Similar to the channel setting and view geometry of AMSR-E, MWRI conically scans the Earth at five frequencies (10.7, 18.7, 23.8, 36.5, 89.0 GHz) and dual (H, V) polarizations. The MWRI has four major differences considering AMSR instruments, including: (a) no C-band channel relative to the AMSR 10.7 GHz channels due to widespread C-band RFI; (b) coarser spatial resolution and slightly narrower orbital swath for all frequencies relative to the AMSR sensors; (c) an approximate 10-min satellite overpass time difference between MWRI and AMSR-E; and (d) an approximate 53-degree earth incident angle (EIA) of measurement instead of 55 degrees for the AMSR sensors. Detailed sensor configurations for AMSR-E, AMSR2 and MWRI are summarized in Table 2.

2.3.3 FY3B-MWRI satellite Images

The FY3 series MWHS is a five-channel cross-track scanning instrument able to provide vertical humidity information to the NWP data assimilation systems. The vertical resolution is poor, with only 2 to 3 pieces of independent information. Nonetheless, this has been proven valuable to NWP in the past.

2.3.4 Soil moisture retrieval using satellite images

The satellite images offer brightness temperature and soil moisture that is affected by vegetation and soil type. Analyzing field survey data and satellite images using regression methods helps to calibrate satellite data. Various algorithms for retrieval of soil moisture from radiometer brightness temperature have been developed, including single channel algorithm (SCA), land parameter retrieval model (LPRM), physically based statistical methodology (PBSM)18, and official algorithms developed by national aeronautics and space administration (NASA) of the United States and Japan aerospace exploration agency (JAXA) according to AMSR-E

Table 1. Some synoptic meteorological stations in the study area

Station name	*Latitudes*	*Longitudes*
Zahedan	29.288318	60.539543
Zabol	31.0127	61.5837
Khash	28.1713	61.1403
Hirmand	31.2187	61.6538
Iranshhar	27.203	60.6853
Chabahar	25.2927	60.6496
Sarbaz	26.6336	61.2568
Saravan	27.7345	62.2627

Table 2. Satellite microwave sensor configurations used in this study

Instrument configurations			
Specifications	**AMSER-2**	**AMSER-E**	**MWRI**
Satellite platform time	GCOM-W1	AQUA	FY3B
(Local time zone)	1:30 p.m. ascending	1:30 p.m. ascending	1:40 p.m. ascending
Antenna Size	1:30 a.m. descending	1:30 a.m. descending	1:40 a.m. descending
incident angle	2 m (Diameter)	1.6 m (Diameter)	0.977 m × 0.897 m
	55	55	53
Spatial Resolution (km×km)			
Band (GHz)	**AMSER-2**	**AMSER-E**	**MWRI**
6.93	62 × 35	75 × 43	N/A
7.3	62 × 35	N/A	N/A
10.65	42 × 24	51 × 29	85 × 51
18.7	22 × 14	27 × 16	50 × 30
23.8	19 × 11	32 ×18	45 × 27
36.5	12 × 7	14 × 8	30 × 18
89	5 × 3	6 × 4	15 × 9

configurations. All these algorithms are based on the same radioactive transfer model. (Omega-tau) which assumes that vegetation multiple scattering and reflection at the air-vegetation interface are negligible. The SCA is basic option for the Chinese FY-3 soil moisture products. Meteorological data such as wind, horizontal visibility, field observation and precipitation data will be used to retrieve Dust storm occurrence and severity.

2.3.5 Satellite image processing

Before using satellite images, the following corrections (Fig. 2) are applicable to the understudied data, depending on some key parameters.

2.3.6 Radiometric correction

Radiometric errors depend on the physical properties of the sensor. Over time, the radiometer will be amortized and, as a result, the sensor will be affected by errors such as distance from the sun, the change in the angle of zenith, and so on, radiometric corrections must be made on the images to resolve these errors. For this purpose, the first step is the conversion of numerical values (DN) to spectral radiation, which is performed using the calibration coefficients of the sensor, and then the amount of spectral radiation calculated is converted into spectral reflection.

$$\%\,\text{Albedo} = (\text{A} * \text{DN}) + \text{B} \qquad \cdots (1)$$

Here, DN is the pixel digital value and A and B are the calibration coefficients of the satellite.

Atmospheric correction involves removing noise in this case clouds and aerial distortions from the images and obtaining reflections from the surface of the earth whiles Geometric corrections eliminates the spatial-spatial errors caused by pixels, the factors causing these errors, the curvature of the earth, the imaging state, the type of satellite view, the post and the heights of the ground, height and speed of the sensor.

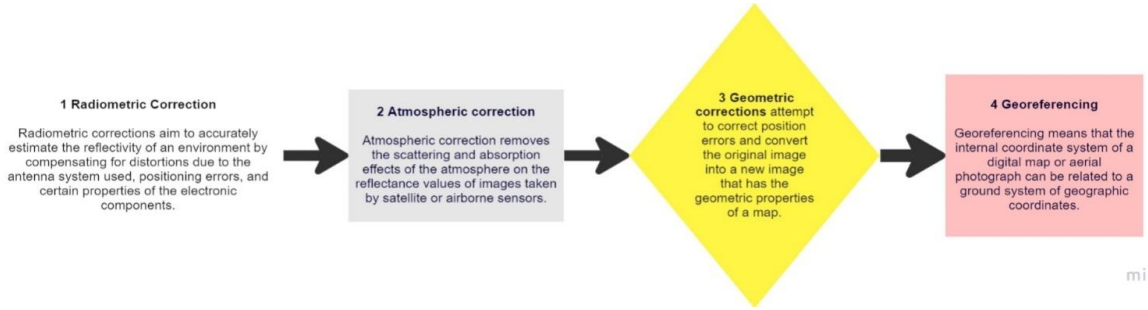

Fig. 2. Conceptual flow of satellite image corrections.
1. Radiometric correction 2. Atmospheric correction 3. Geometric correction 4. Georeferencing

AMSR-E / Aqua Daily L3 Surface Soil Moisture, Interpretive Parameters, and QC EASE-Grids are combined and soil moisture is globally and in terms of obtained. Then, these data were geo-reference and soil moisture was extracted in Iran and by Khorasan Razavi province for 2009.

2.4 Data Analysis

2.4.1 Comparison of the degree of soil brightness in dry and wet conditions

The amount of energy received by the sensor, which determine by the brightness (DN) of the images, is converted to the brightness temperature using the inverse of the Planck function and based on the following relationships. Figs. 3 and 4 shows difference in the brightness of the DN4-DN5 bands and the brightness of the bands of the BT4-BT5 bands show quite dry and perfectly wet conditions after atmospheric conditions.

As it is seen, the values obtained from the soil surface in dry soil conditions range from (-5 to -13), whereas that of humid conditions range from (8 to 10).

2.4.2 Quantity of albedo in different humidity conditions using reflective bands

Soil texture in the study area is determined using the global database, the amount of albedo has been determined in different conditions, and the final calibrated results have been determined. An example of the calibration coefficients presented in the global database of NOAA: Table 3.

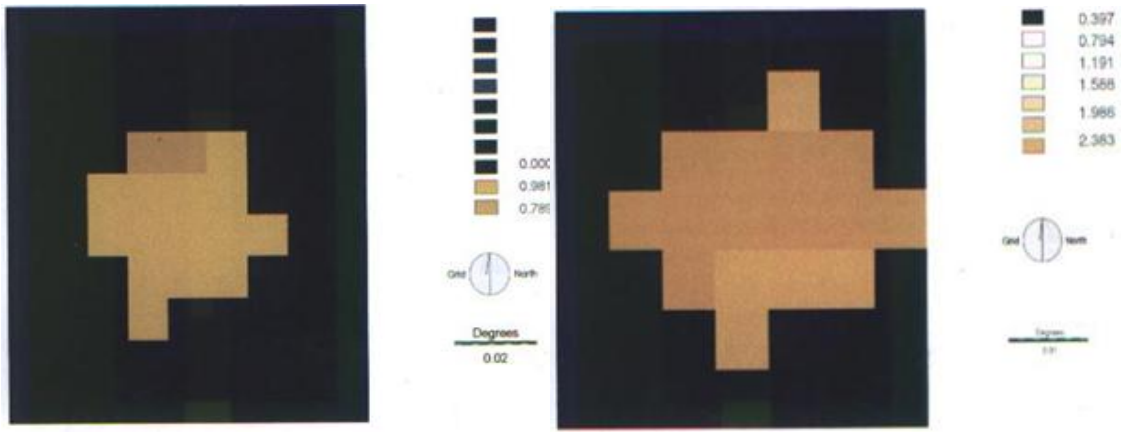

Fig. 3. Differences between degrees of lighting in wet and dry soil- DN4-DN5 bands

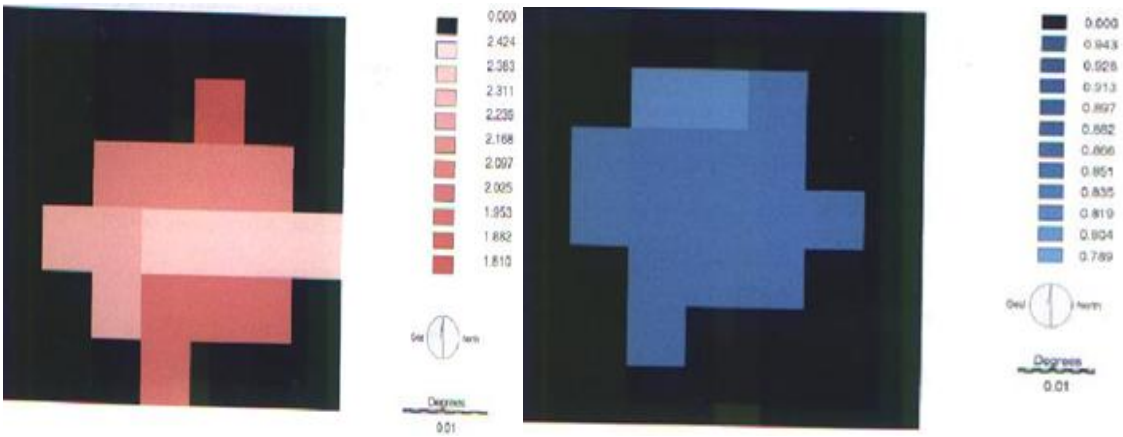

Fig. 4. Differences in thermal band (BT4-BT5) temperatures in wet and dry conditions

Table 3. Bands, slope and intercepts

Band	Slope	Intercept
b_1	0/1081	-3/8648
b_2	0/1090	-3/6749

$$B1 = -\frac{3}{8648} + \frac{0}{1080} - b_1 \quad \ldots(2)$$

$$B2 = -\frac{3}{6749} + \frac{0}{1090}\ b_2 \quad \ldots(3)$$

Based on the above relations, the amount of albedo in each pixel, such as the ground, it calculated according to the different soil moisture conditions, and then the average albedo obtained is determined as the desired pixel albedo.

2.4.3 Estimation of moisture content for soil surface layer (in grams per cubic centimeter)

In order to estimate the surface soil moisture, brightness temperature, the surface temperature, the albedo of each image pixel and its equivalent were calculated in the specified period. The obtained data were in grams per cubic centimeter changed to volume unit (percent) to be analyzed. The soil moisture content defined as the ratio of the water weight in the soil mass to the weight of its solid components (Abshoori, 1377). We had two scans for every point per day for a 12-hour interval. One scan was randomly selected. There have been 360 scans in one year for the entire area under study (Khorasan Razavi province).

To convert mass moisture to volumetric moisture, it is required to have the particle density of the soil in that region per cubic centimeter. The soil particle density is defined as the weight of soil in a given volume (g/cm3) (Nouroozi et al. 1387). The space between particles is not associated with the particle density. The particle density of the soil ranges from 2.60 to 2.75 g/cm^3. This value is almost constant, since most of the minerals existing in the soil have the similar density. The soil density exceeds 2.75 in the presence of such mineral's tourmaline, magnetite and hornblende. Organic materials are lighter than minerals. Therefore, soils that contain relatively large amounts of organic matter have lower particle density, and according to this principle, the particle density of surface soil is always lower than that of the soil below the surface of the ground.

$$D' = \left(\frac{P'}{V'}\right) \quad \ldots(4)$$

D: Bulk density in g/cm^3
V': Volume of dried soil in 105°C in a normal condition in terms of cm^3
P': Weight of dry soil in 105°C in a normal condition in terms of g.

According to the particle and bulk density of the soil and by using the following formula, the soil porosity is calculated:

$$The\ soil\ porosity = 100 - (particle\ density|bulk\ density) \times 100 \quad \ldots(5)$$

The soil must have appropriate porosity for water and aeration. The percentage of soil volume occupied by solid matters is equal to the ratio of bulk density to particle density, multiplied by 100.

Finally, it is necessary to mention that new information sources and optimized methods have been effective in estimating and measuring surface soil moisture. One of these methods is use of AMSER-E, which provides processing, and correction of the data, extraction and evaluation of such indexes as soil temperature, brightness temperature by using separate bands and the soil surface albedo through performance of difference steps.

3. RESULTS

To accurately determine the areas affected by dust storms and understand the dispersion of dust particles in the Sistan region, satellite image processing is utilized. It is crucial to acquire images that can cover the entire region of interest, as dust storms have a significant spatial extent and can transport particles over long distances. Thus, the identification of these storms requires high-coverage and highly repeatable images. The MODIS 1 sensor on board the TERRA satellite is particularly suitable for this purpose. In addition to its wide coverage and repeatability, the sensor captures a broad range of radiant energy across visible and invisible spectral ranges, enabling effective analysis and identification of dust storms in the region.

3.1 Dust Density in 2014

The dust intensity map (Fig. 5) is a product that has been generated by applying a dust monitoring and processing model of over 2053 MODIS satellite imagery with a resolution of 10 km in 2014 (daily). This monthly average map shows the intensity of the dust in each area. Also, due to the comparison of the results with ground stations, the values of the intensity above the chosen threshold represent the phenomenon of dust and, as much as it is added, the phenomenon of dust in the region will be more severe.

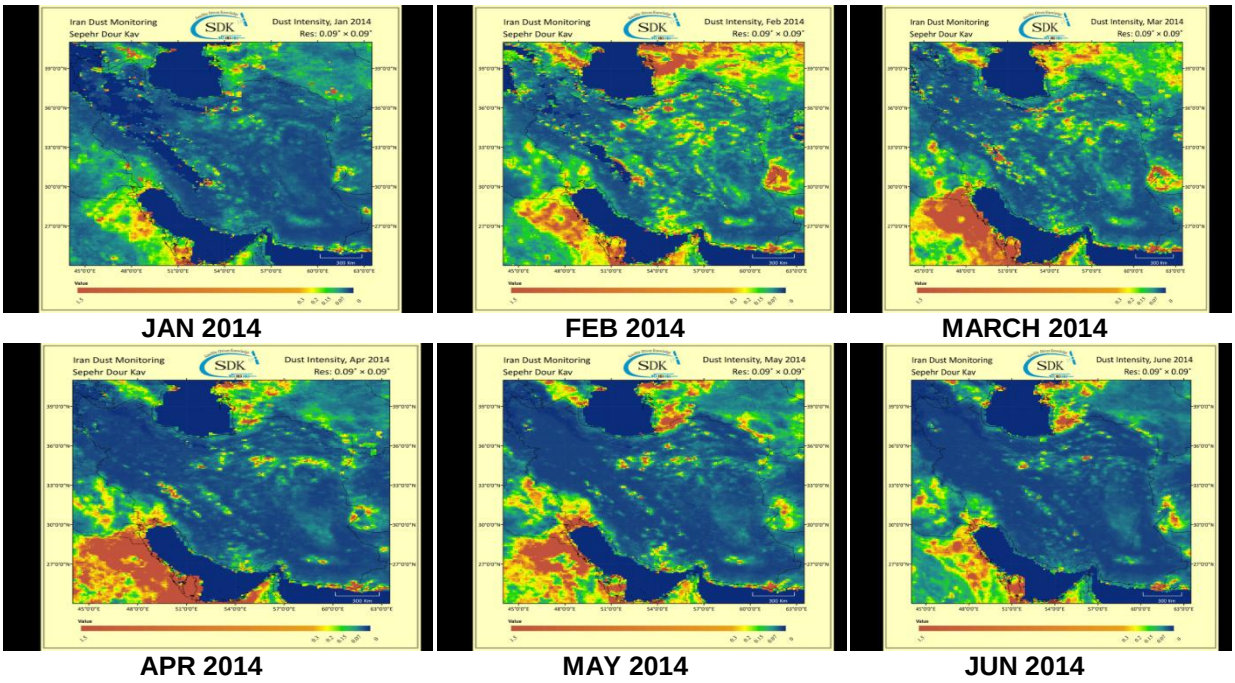

Fig. 5. 2014 Dust density maps of the study domain

3.2 Dust Intensity for 2017

The dust intensity map is a product that has been generated by applying a dust monitoring model and processing more than 979 MODIS satellite imagery with a resolution of 10 km in 2017 (on a daily basis). This monthly average map shows the intensity of the dust in each area (Fig. 6). Also, due to the comparison of the results with ground stations, the values of the intensity above the chosen threshold represent the phenomenon of dust and, as much as it is added, the phenomenon of dust in the region will be more severe.

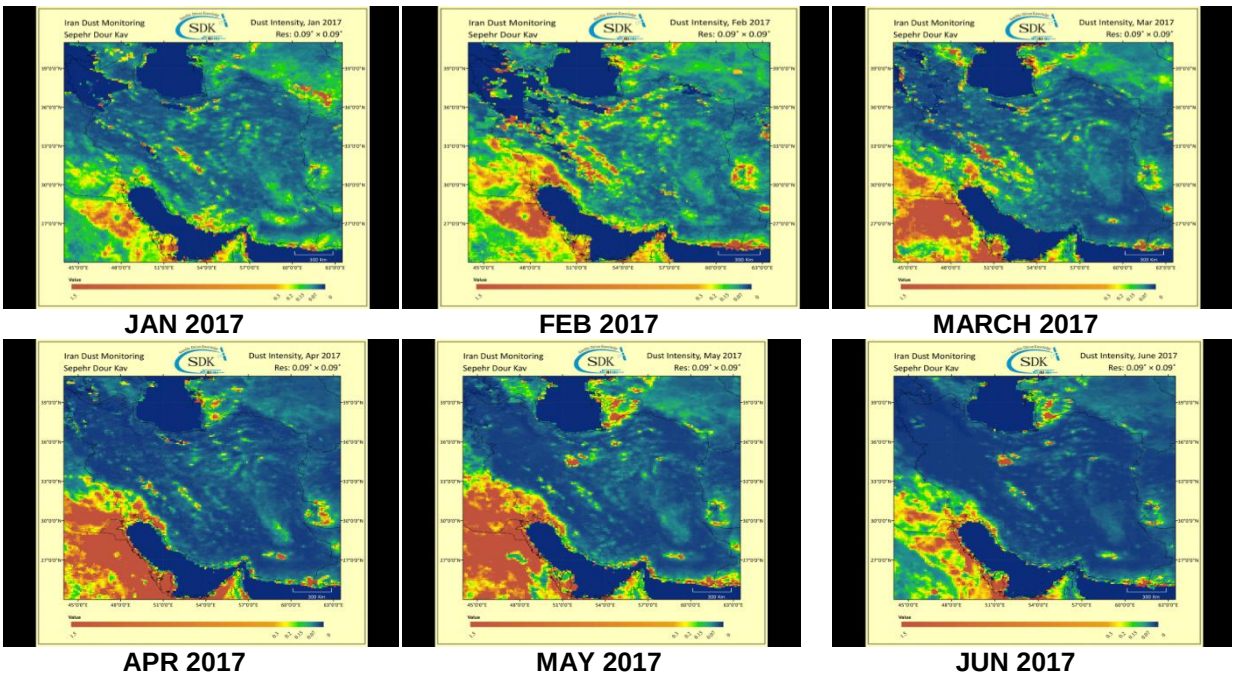

Fig. 6. 2017 dust density maps

3.3 Investigation of Soil Moisture Changes in Relation to Dust Storms

At this stage, we plan to investigate the changes in soil moisture in the dates of the occurrence of dust. Therefore, we will draw up the moisture maps for the last few days and then examine the process of change.

3.4 Land Surface Soil Moisture Maps for 2017

Fig. 7 shows the land surface's soil moisture for the given study period; thus, between June 22 and July 3, 2017.

3.5 Parametric Monitoring of Dust Events

The combination of wind parameters and soil moisture has a great influence on the formation of dust in a particular region. In this way, as the amount of soil moisture decreases and the wind speed increases, the probability of a dust phenomenon also increases. This problem is more common in areas with poor vegetation than in other areas. The following figures show the state of soil moisture and the intensity of daily dust in the Sistan and Baluchestan region of southeastern Iran, and the graph shows the status of wind speed, soil moisture and dustiness or absence of specific days from 2015, 2016 and 2017 (Figs. 8 and 9). Comparing the situation on 23/04/2016 and 07/04/2017, or 12/06/2016 and 16/09/2016, it can be concluded that at the same wind speed, an increase in the percentage of soil moisture can be due to the occurrence of the event prevents dust. Therefore, the long-term correlation between these two parameters with the occurrence of dust storms can be found in extracting the threshold limits of these variables to create dust storms.

Table 4. Major dust storm events in the study area

Relevant dates	Type of phenomenon	Place of occurrence
June 22 to July 3, 2017	Dust storm	Sistan and Baluchestan province
26 to 29 April 2017	Dust storm	Sistan and Baluchestan province
30 September to 4 October 2016	Dust storm	Khuzestan

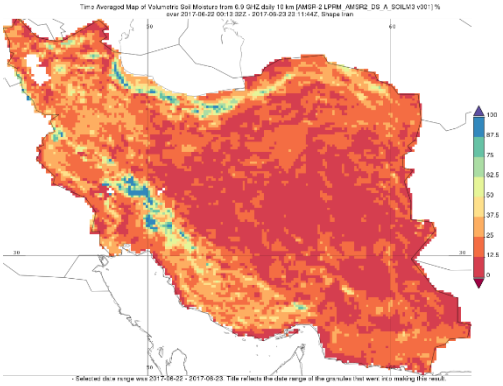

22-Jun-2017-Ascending

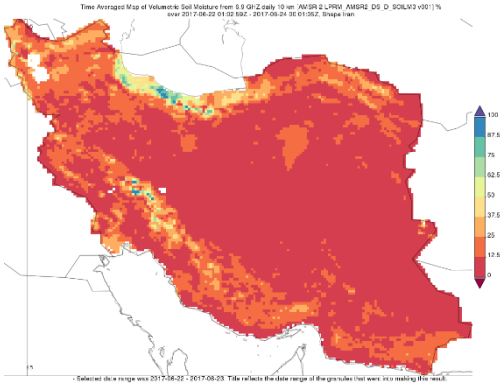

Descending-22-Jun-2017

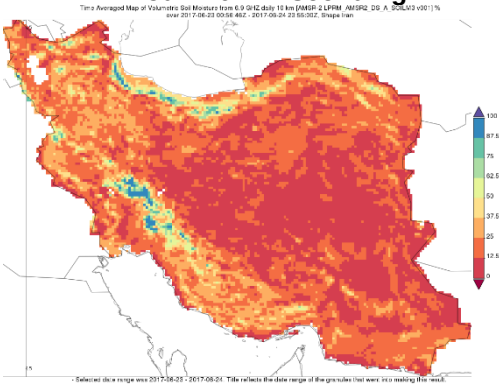

23-Jun-2017-Ascending

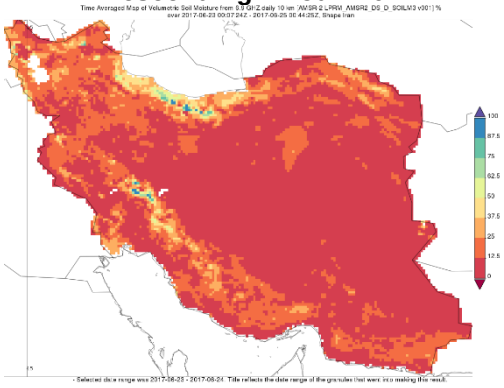

Descending-23-Jun-2017

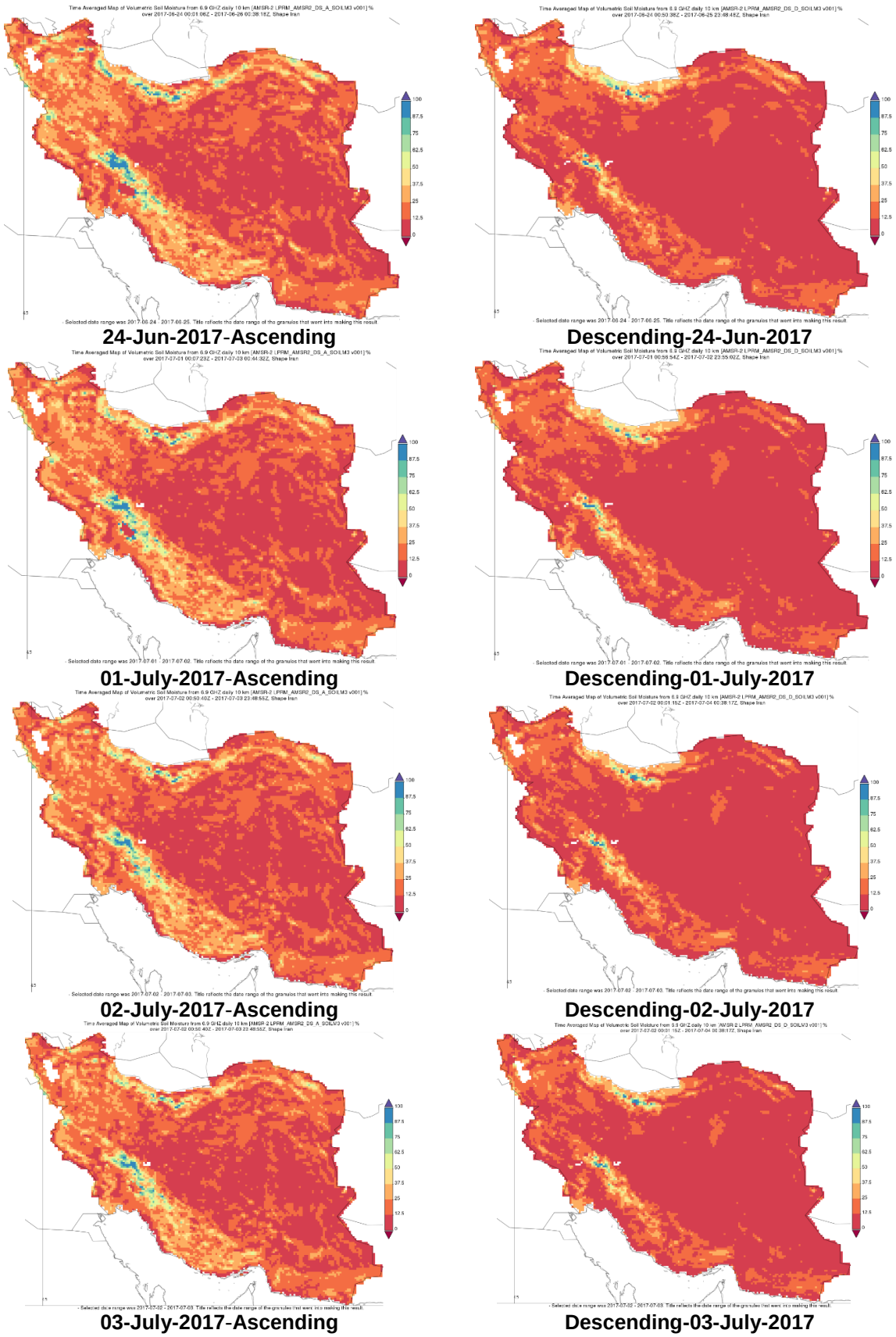

Fig. 7. Time averaged map of soil moisture from 6.9GHZ daily 10 km (AMSER-2)-IRAN

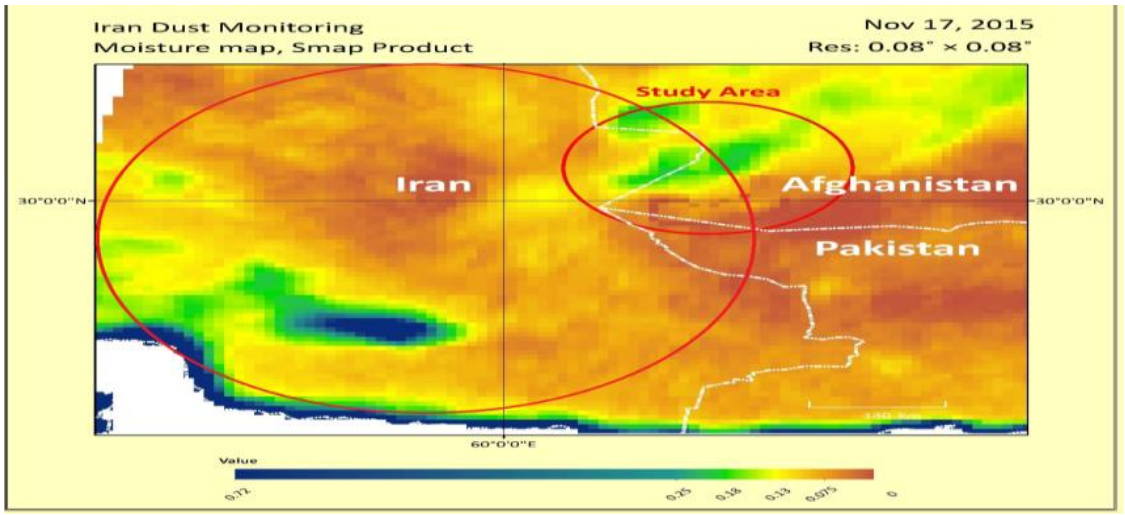

Fig. 8. Soil moisture map extracted from SMAP images with a resolution of 9 km - The small red circle indicates the origin of the dust and the studied area

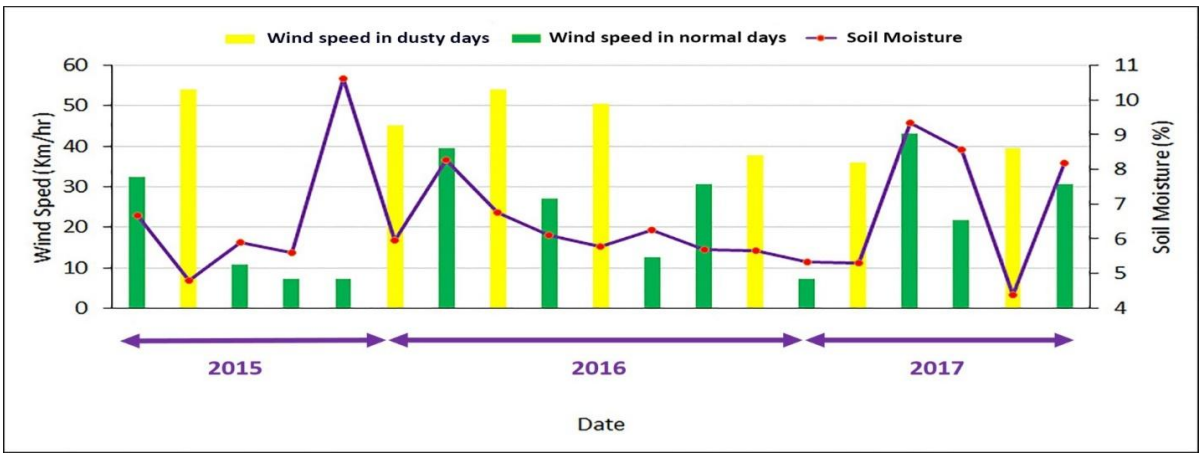

Fig. 9. Wind speed and soil moisture diagram

Combination of wind speed and soil moisture diagram - yellow diagram showing the events of the dust and the green diagram indicating the days without dust - Increasing the moisture content of the wind with the same wind speed, in most cases preventing the storm of dust.

3.6 The Relationship between Soil Moisture Content and Dust Concentration

Table 5 shows the amount of soil surface moisture content and the density of the dust in the understudied areas.

Table 5 shows the relationship between soil surface moisture content and the density of the dust of the studied areas. As is clear, the concentration of released dust on the soil surface has decreased with increasing relative humidity. Detection of the rate of decline for different regions of the soil is different, but all soils have fallen sharply in humidity by 2.2% and are approaching zero.

Therefore, we can say that at a humidity point of 2.2%, inter-particle forces have the greatest effect on the moisture content of the surface soil to increase adhesion between soil particles.

Evidence presented above (Fig. 10) indicates dry soil (humidity near zero) has the highest dust production rate of 168.66 mg / m3. This amount is more than 10 times the standard human standard (15 mg / m^3)[1]. With increasing humidity from zero to about 3%, the amount of dust released has dropped.

[1] *Global health website*

Table 5. Amounts of soil surface moisture content and the density of the dust of the studied areas

RH	density	RH	density
50	40	5.6	110
39	45	5.4	115
28	50	5.2	120
17	55	4.2	125
15	60	3.2	130
13.8	65	2.1	135
12.6	70	1.1	140
11.4	75	1	145
10.2	80	0.9	150
9	85	0.9	155
7.8	90	0.8	160
6.6	95	0.7	165
6	100	0.7	170
5.9	105		

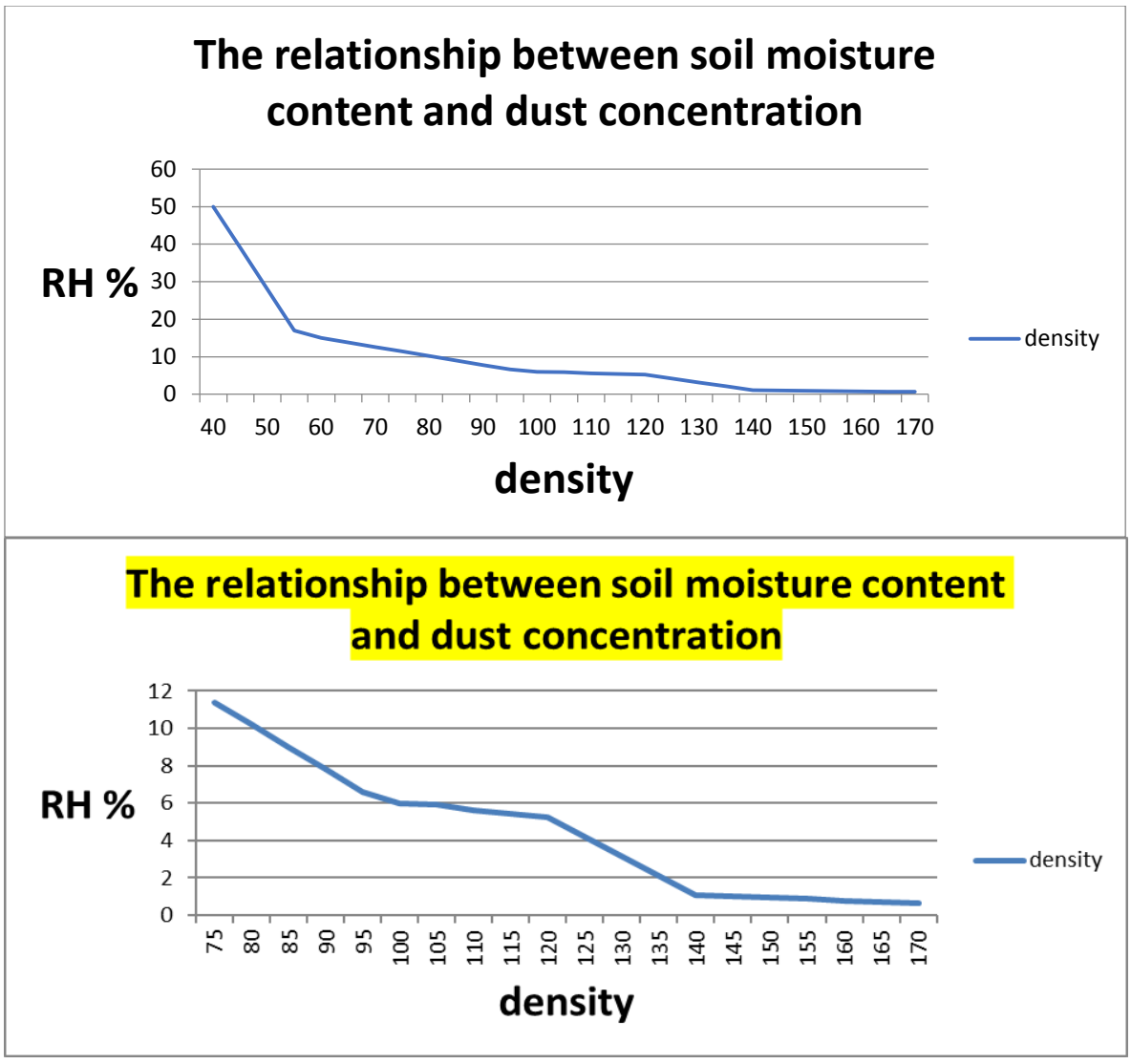

Fig. 10. The relationship between soil moisture content and dust concentration

3.7 Validation of Error Estimation of Satellite Soil Moisture

In order to study the accuracy of soil moisture retrievals in the study areas, soil moisture data of AMSER-E and FY-3 and ground data (weather stations) were evaluated using various statistical indices. In order to verify the surface moisture content obtained from the microwave data, the correlation of Zabol and Zahedan cities with surface moisture content obtained in two AMSER-E and FY-3 satellites was investigated. Table 6 clearly shows correlation coefficient of surface moisture content obtained on AMSER-E satellite of Zabol and Zahedan cities.

Table 7 clearly shows correlation coefficient of surface moisture content obtained on FY-3 satellite of Zabol and Zahedan cities.

In this section, the correlation of humidity between Zahedan and Zabol stations was investigated with surface moisture content obtained from the E-AMSR and FY-3 sensors. The results show a significant correlation between surface and satellite surface moisture at 90% and 95% confidence levels.

Correlation coefficient in AMSER-E satellite is not significant only at Zahedan station in 2014 and correlation coefficient at Zahedan station in 2016 and at Zabol station in 2017 is not significant at 95% level. This correlation between surface and surface water content data shows the adequacy of these data and confirms the usefulness of using such wide area coverage data in water and soil research.

4. DISCUSSION

Soil moisture quantification across the entire region, is known to be one of the most challenging environmental indices which has been observed to be very important, yet difficult to quantify. In establishing the various findings of this study, the MODIS data points out that there is generally severe dust in this region of study. Monthly average dust observations of 2014 through to 2017 depict high dust over the area (Pour Kermani, 1365). Table 4 shows the major dust event dates between some specific wind parameters and soil moisture. These parameters have great influence on the formation of dust in the study domain. Findings revealed as the amount of soil moisture decreases, whilst the wind speed increases, the probability of a dust phenomenon also increases as revealed by (Salvucci et al., 2002). This could be attributed to the poor vegetation of the area. In 2017, as shown in Fig. 7, soil moisture varied from 6.9GHZ daily with every 10 km using the (AMSER-2) in southeastern Iran.

Table 6. Correlation coefficient of Zabol and Zahedan cities against surface moisture content on AMSER-E satellite

	ZABOL			ZHAHEDAN		
Year	**The correlation coefficient**	**90% level**	**95% level**	**The correlation coefficient**	**90% level**	**95% level**
2013	0.363	+	+	0.517	+	+
2014	0.460	+	+	0.204	-	-
2015	0.509	+	+	0.330	+	+
2016	0.330	+	+	0.296	+	+
2017	0.688	+	+	0.431	+	+

Table 7. Correlation coefficient of Zabol and Zahedan cities against surface moisture content of on FY-3 satellite

	ZABOL			ZHAHEDAN		
Year	**The correlation coefficient**	**90% level**	**95% level**	**The correlation coefficient**	**90% level**	**95% level**
2013	0.606	+	+	0.738	+	+
2014	0.821	+	+	0.78	+	+
2015	0.561	+	+	0.744	+	+
2016	0.734	+	+	0.419	-	-
2017	0.51	+	-	0.746	+	+

Correlation analysis between wind speed and soil moisture is displayed in Fig. 9. Based on evidence presented in Fig. 9, an inverse relationship between wind speed and soil moisture between 2015 and 2017 period could be observed. Here, increasing moisture content of the wind along the speed of the wind prevents the formation of dust storms and this is clearly confirmed by (Holcombe et al., 1997). Over the study period, the three different months studied revealed precipitation varied; thus, 30mm, 6mm and 4 mm in 2015, 2016 and 2017 respectively. Table 5 presents the relationship between soil surface moisture content and the density of dust in the study region. The concentration of released dust on the surface of the soil has decreased with increasing relative humidity. Detection of the rate of decline for different regions varies; however, results prove all the soils have sharply reduced in relation to humidity by 2.2%, approaching the zero margins.

Moreso, we further validated the error estimation of the satellite's soil moisture. Tables 6 and 7 shows the correlation of humidity between Zahedan and Zabol ground-based stations and satellites. These were investigated using surface moisture content obtained from the E-AMSR and FY-3 sensors. The results show a significant correlation between surface and satellite surface moisture at 90% and 95% confidence levels (Ravi et al., 2004; Natsagdorj et al., 2003; Wang et al., 2004; Ishizuka et al., 2005; Tegen et al., 2004; Cowie et al., 2013). Based on these findings, we can conclude that there was a strong correlation between soil moisture content as measured by AMSR-E and rainfall data in the study area. Correlation coefficient in AMSER-E satellite was insignificant at Zahedan station in 2014. Again, the correlation coefficient of Zahedan station in 2016, and that of Zabol station in 2017 was also not significant at 95% confidence level. The association of surface and surface water content data shows the adequacy of these datasets, which confirms the usefulness of using such wide area coverage data in water and soil research.

The varying nature of soil moisture makes it a daunting task in quantifying it in a spot or field across a sizable region in hydrological and climatological studies. MODIS datasets which were plainly tagged as inappropriate for such measurements or studies of this nature were used. Additionally, the datasets used which encapsulated minor errors were scaled or normalized to enhance the study's validity and reliability in drawing logical conclusions. Further studies could consider technological developments or strategies for accurate recording of data and measurements of discrepancies in soil moisture measurements, as shown in the present study that soil moisture despite its environmental relevance varies across space.

5. CONCLUSION

The accuracy assessment and accuracy of surface soil moisture data at large spatial scales is essential for careful and accurate environmental surveys. Now we can conclude that direct measurement of soil moisture and the extraction of moisture data in a point is not only costly and time-consuming, but on a large scale, it is not practical. Despite the importance of soil moisture in environmental studies, due to the cost and time consuming of spot measurements, this parameter is not widely used in climatic models. Due to the lack of availability of long-term soil moisture data at Iran's meteorological stations, microwave satellite data is used due to its continuous measurements of the surface of the earth, ability to record physical properties of different coatings on the ground and long-term archives are a good substitute for soil moisture spot measurements. By using satellite data, it is possible to prepare time and spatial distribution of relative humidity of soil in networks ranging from 500 m to 20 km depending on the type of sensor. Among the key highlights or relevance of this research is that, when considering the capabilities of the AQUA satellite for measuring soil moisture and its adaptation to the climatic realities of Iran, the moisture content extracted from the satellite and the precipitation status of Khorasan province in the understudied stations were checked to ensure that the AMSER and FY-3 satellite data have high accuracy.

Therefore, it is possible to use the data of these satellites to evaluate drought monitoring, hydrology, weather and forecasting of storm and dust. Similarly, its applicability is essential in the agriculture and natural resource management sectors for modelling and soil moisture assessment purposes. Overall, it can be concluded that soil moisture retrievals are well-matched in comparison to the measured data at study stations. Lack of soil moisture data in most parts of Iran is always a major problem in hydrological modeling, meteorological forecasting and water resource management and planning. Therefore, based on the results of this

study, soil moisture estimates can serve as a suitable tool for preparing soil moisture maps and the evaluation of temporal and spatial variations of soil moisture in study region to address issues related to dust storms.

In this research, the utilization of satellite images for determining the center of storms and tracking their movement has been evaluated as highly appropriate. Besides the external factors contributing to the formation of storms in the Sistan region, a significant portion of them can be attributed to the decrease in surface soil moisture within the region. Consequently, it appears essential to devise a dual-pronged approach when planning measures to mitigate dust storms and minimize their associated damages. Firstly, efforts should be made to control dust storms originating from the surface of Hamon Saburi lake, if feasible, given its status as the primary source area. Secondly, protective measures such as implementing vegetation establishment plans should be implemented to prevent the escalation of dust concentration along transportation routes.

DATA AVAILABILITY

The data that backs up the study's conclusions is accessible and will be supplied upon request.

ACKNOWLEDGEMENTS

The authors would like extend their profound gratitude to the Institute of Remote sensing at the Nanjing University of Information Science and Technology for providing the needed resources for the accomplishment of this project.

COMPETING INTERESTS

Authors have declared that no competing interests exist.

REFERENCES

1. Akbari M, Toomanian N, Droogers P, Bastiaanssen W, Gieske A. Monitoring irrigation performance in Esfahan, Iran, using NOAA; 2007.
2. De Ridder K. Quantitative estimate of skin soil moisture with the Special Sensor Microwave/Imager. Boundary-Layer Meteorol. 2000;96:421-432.
3. Draper C, Walker J, Steinle P, de Jeu R, Holmes T. An evaluation of AMSR–E derived soil moisture over Australia, Remote Sensing of Environment. 2009; 113(4):703-710.
4. Marshall GS. Drought detection and quantification using field-based spectral measurements of vegetation in semi-arid regions. New Mexico Institute of Mining and Technology Department of Earth and Environmental Science; 2005.
5. Mattia F, Satalino G, Pauwels VRN, Loew A. Soil moisture retrieval through a merging of multi-temporal L-band SAR data and hydrologic modeling. Hydrology and Earth System Sciences. 2008;5:3479–3515.
6. Moran MS, Peters-Lidard CD, Watts JM, McElroy S. Estimating soil moisture at the watershed scale with satellite-based radar and land surface models, Can. J. Remote Sens; 2004.
7. Narasimhan B, Srinivasan R. Development and evaluation of Soil Moisture Deficit Index (SMDI) and Evapotranspiration Deficit Index (ETDI) for agricultural drought monitoring. Agricultural and Forest Meteorology. 2005;133:69–88.
8. Palmer WC. Meteorological Drought. Research Paper No. 45, US Weather Bureau, Washington, DC; 1965.
9. Peñuelas J, Piñol J, Ogaya R, Filella I. Estimation of plant water concentration by the reflectance water index WI (R900/R970). International Journal of Remote Sensing. 1997;18:2869−2875.
10. Jiancheng Shi, Yang Du, Jinyang Du, et al. Progresses on microwave remote sensing of land surface parameters, Science China: Earth Sciences. 2012;55(7):1052-1078.
11. Shi J, Jiang LM, Zhang LX, et al. Physically based estimation of bare surface soil moisture with the Passive Radiometers, IEEE Transactions on Geoscience and Remote Sensing. 2006; 44(11):3145- 3153.
12. Jackson TJ, Le Vine DM, Hsu AY, et al. Soil moisture mapping at regional scales using microwave radiometry: The Southern Great Plains Hydrology Experiment, IEEE Transactions on Geoscience and Remote Sensing. 1999;37(5):2136-2151.
13. Akbari M, Toomanian N, Droogers P, Bastiaanssen W, Gieske A. Monitoring irrigation performance in Esfahan, Iran, using NOAA; 2007.
14. De Ridder K. Quantitative estimate of skin soil moisture with the Special Sensor

Microwave/Imager. Boundary-Layer Meteorol. 2000;96:421-432.
15. Peters AJ, Rundquist DC, Wilhite DA. Satellite detection of the geographic core of the 1988 Nebraska drought. Agricultural and Forest Meteorology. 1991;57:1-3.
16. Rao S, Sharma V, Garg, Venkataraman G. Soil Moisture Mapping over India using Aqua AMSR-E derived Soil Moisutre Product, Proceedings of the IEEE International Conference on Geoscience and Remote Sensing Symposium, Denver, USA. 2006:2999-3002.
17. Wigneron JP, Schmugge T, Chanzy A, Calvet JC, Kerr Y. Use of passive microwave remote sensing to monitor soil moisture a review, Agronomie: Agriculture and Environment. 1998;18:27-43.
18. Wilhite DA, Buchanan-Smith M. Drought as Hazard: Understanding the natural and social context. In Drought and Water Crises Science, Technology, and Management Issues. Edited by Donald A. Wilhite. Taylor & Francis Group; 2005.
19. Hu Yang, Naimeng Lu, Zhiqiang Ge, et al. The microwave sensor status and future developing plan of China meteorological satellites, Proc. SPIE 7452, Earth Observing Systems. 2009;XIV:745213. DOI: 10.1117/12.833758
20. Marshall GS. Drought detection and quantification using field-based spectral measurements of vegetation in Semi-Arid Regions. New Mexico Institute of Mining and Technology Department of Earth and Environmental Science; 2005.
21. Mattia F, Satalino G, Pauwels VRN, Loew A. Soil moisture retrieval through a merging of multi-temporal L-band SAR data and hydrologic modeling. Hydrology and Earth System Sciences. 2008;5:3479–3515.
22. Narasimhan B, Srinivasan R. Development and evaluation of Soil Moisture Deficit Index (SMDI) and Evapotranspiration Deficit Index (ETDI) for agricultural drought monitoring. Agricultural and Forest Meteorology. 2005;133:69–88.
23. Palmer WC. Meteorological Drought. Research Paper No. 45, US Weather Bureau, Washington, DC; 1965.
24. Peñuelas J, Piñol J, Ogaya R, Filella I. Estimation of plant water concentration by the reflectance water index WI (R900/R970). International Journal of Remote Sensing. 1997;18:2869−2875.
25. Peters AJ, Rundquist DC, Wilhite DA. Satellite detection of the geographic core of the 1988 Nebraska drought. Agricultural and Forest Meteorology. 1991;57:1-3.
26. Rao S, Sharma V Garg, Venkataraman G. Soil Moisture Mapping over India using Aqua AMSR-E derived Soil Moisutre Product, Proceedings of the IEEE International Conference on Geoscience and Remote Sensing Symposium, Denver, USA. 2006;2999-3002.
27. Wang X, Xie H, Guan H, Zhou X. Different responses of MODIS-derived NDVI to root-zone soil moisture in semi-arid and humid regions. Journal of Hydrology. 2007;340: 12–24.
28. Wigneron JP, Schmugge T, Chanzy A, Calvet JC, Kerr Y. Use of passive microwave remote sensing to monitor soil moisture a review, Agronomie: Agriculture and Environment. 1998;18:27-43.
29. Wilhite DA, Buchanan-Smith M. Drought as Hazard: understanding the natural and social context. In Drought and Water Crises Science, Technology, and Management Issues. Edited by Don; 2005.
30. Sobhani B, Salahi B, Goldost A. Study the dust and evaluation of its possibility prediction based on statistical methods and ANFIS model in Zabol university. Geography and Developemnet. 1391;38: 123-138.
31. Khoddam N, Ahamadi Givi F, Iran Nejad P. Climatological effects of the Indian monsoon in Iran. Master's thesis, Geophysics Institute, Teharan University; 1391.
32. Khoddam N, Iran Nejad P, Ahamadi Givi F. A study of the impact of Indian Monsoon on Summer Climate of Iran. Iran Geophysics J. 1394;9(2):52-66.
33. Rashki A, Kaskaoutis DG, deW CJ, Rautenbach PG, Eriksson M, Qiang, Gupta P. Dust storms and their horizontal dust loading in the Sistan region, Iran. Aeolian Research. 2012;5:51-62.
34. Mofidi A, Hamidian Pour M, Salighe M, Alijani B. Determination of the Onset, Withdrawal and Dusation of Sistan Wind Using a Ckange Point Approch. Geography and environmental Hazards. Winter. 1392,2014;2(8):87-112.
35. Alizadeh-choobari O, Zawar-Reza P, Sturman A. The wind of 120 days and dust storm activity over the Sistan basin. Atmos. Res., 143, 328-341.WMO Airborne dust bulletin. 2014;1(2017).

36. Sehatkashani S, Sedaghatkerdar A, Bidokhti AA, Gh A Kamali, Ranjbar A, Salehi M. The NumericalEvaluation of Low-level Jets Formation in Lut Valley Region in Winter, envoc Health 2009, India; 2009.
37. Prospero JM, Ginoux P, Torres O, Nicholson SE, Gill TE. Environmental characterization of global sou7rces of atmospheric soil dust identified with the nimbus 7 total ozone mapping spectrometer (TOMS) absorbing aerosol product. Rev. Geophys. 2002;40(1): 1002.
DOI: 10.1029/2000000095
38. Sehatkashani S, Bidokhti AA, Ranjbar A. Numerical study of wind field in Lot valley using umerical simulation in two hot and cold seasons. Master's thesis, Meteorology department, Faculty of science, Islamic Azad University Science and Research Branch; 1385.
39. Kaskaoutis DGA, Rashki EE, Houssos A, Mofidi D, Goto A, Bartzokas P, Francois, Legrand M. Meteorological aspects associated with dust storms in the Sistan region, southeastern Iran. Clim. Dyn. 2014;45:407–424.
40. Kaskaoutis DG, Houssos EE, Rashki A, Francois P, Legrand M, Goto D, et al. The Caspian Sea-Hindu Kush index (CasHKI): A regularity factor for dust activity over southwest Asia. Global and Planetary Change. 2016;137:10-23.
41. Mc Tainsh G, Tews K. Soil erosion by wind - Dust Storm Index (DSI): National Monitoring and Evaluation Framework, prepared for the National Land and Water Resources Audit, Canberra; 2007.
42. Kalnay E, Kanamitsu M, Kistler R, Collins W, Deaven D, Gandin L, et al. The NCEP/NCAR 40- Year Reanalysis Project. Bull. Amer. Meteor. Soc. 1996;77:437–471.
43. Wang B, Fan Z. Choice of South Asian summer monsoon indices. Amer. Meteor. Soc. 1999;80:629-638.
44. Webster PJ. The Elementary Monsoon. John Wiley, New York, 1987;332.

Peer-review history:
The peer review history for this paper can be accessed here:
https://www.sdiarticle5.com/review-history/102580